The power law scaling, geometric and kinematic characteristic of faults in the Northern part of the Kerman Coal Province (KCP), Iran

Hasan Mansouri[1], Amir Shafiei Bafti*[2], Mohsen Pourkermani[1]

1. Department of Geology, North Tehran Branch, Islamic Azad University, Tehran, Iran
2. Department of Geology, Zarand Branch, Islamic Azad University, Zarand, Iran

Abstract

According to numerous studies, there are basic and initial scaling relationship for the geometric and kinematic characteristics of faults. The study area is located in the northern part of the Kerman coal province. The statistical calculations are consisting of: measure the surface density of faults per unite area and division of the area, determining the direction of the dominant faulting and evaluating the relationship between length-displacement, strike-displacement and strike-length. Based on diagrams, the highest fracture density is related to the middle portion (B zone) of study area because that enclosed between the four main faults and sandstone rock assemblage. The relationship between strike-length parameter is calculated as ($y=0.0478x + 11.54$), and R-squared rate is ($R=0.341$), strike-displacement is calculated as ($y=2.68x + 147.4$) and R-squared rate is ($R=0.65$) and length-displacement is calculated as ($y= 243.58 \ x^{0.0336}$) and R-squared rate is ($R=0/022$). It was determined that increasing the density of fractures and faulting in the study area can be attributed to the complex geological structure, the formation of initial faults and long term progressive deformation. Due to deformations accumulation and formations of multiple structures (like faults, folds and shear zones), have Increasing the fracture density, and topography, and has interacted with together. Comparison the length-strike and strike-displacement parameters, represents a similarity on the clustering in the plotted data Despite that they have many similarities to each other, does not show a dependable dependence, this may indicate their asynchronous creation.

Keywords: *Kerman coal province, Statistical analysis of faults, Scaling relationship, Faulting density.*

1. Introduction

Considering new investments for exploration of coal mines in Kerman, the feasibility of reserves and their productivity are great importance. In this regard, fault structures and their kinetic and statistical geometric characteristics are a decisive factor in the productivity of coal reserves. Therefore, in this study, we tried to understand the kinematic, geometric and statistical characteristics of faults in the north of Kerman coal province. Mechanical controls affecting on formation, growth and expansion of structures (such as joints, faults, veins, etc.) can be examined by statistical analyzing of geometric properties. Structures during the progressive strain are developed by many key features that create generalized scalar relationships in a specific place and in a set of specific sets. The relationships between the geometric properties of structures are described to delineate the mean or long-term equilibrium value or the results of short-term processes occurring which specific spatial scales (For example Kim et al. 2004). Studies show that a subset of variables (such as previous fractures and geological activity rate) has a primary effect on such as length, displacement, strike scaling (For example: Schultz et al. 2013). Main aspects of loading and growth conditions, have been taken strain aggregation during the growth of structures and the evolution of the mechanical properties of rocks.

----
*Corresponding author.
E-mail address (es): kalamus51@hotmail.com

Comprehensive studies show that there are basic and initial scaling relationship for faults such as displacement versus tension (Kim and Sanderson 2005), shear zone width versus displacement (Childs et al. 2009; Aydin and Berryman 2010) geometry of the fault scarp (separation versus overlapping) (Aydin and Nur 1982; Soliva and Benedicto 2004; Long and Imber 2011), displacement and segmentation (Wesnousky 1988; De joussineau and Aydin 2009). The purpose of these studies, in addition to obtaining the relationship between lengths, strike, displacement parameters, is to predict the relative magnitude of each parameter in order to explore the future coal resources and the evolution and synchronization mode and the asynchronous formation of faults.

2. Geological setting

The studied area is located in central Iran and in the northern part of the coal province of Kerman (KCP), which is known as the Kerman coal syncline (Technoexport 1969) (Fig 1A, 1B and 1C). The KCP folded-faulted region is limited from the south to the Urmia- dokhtar magmatic belt, from the north to Ravar-Kalmarad highlands, from the northwest to the Bahabad-Saghand mountain (1B) and from the east and southeast to Lakarkouh mountain. Also is bounded in the western and eastern margin by the Kouhbanan basement fault and the Behabad- Tarz fault respectivly (Fig 1D).
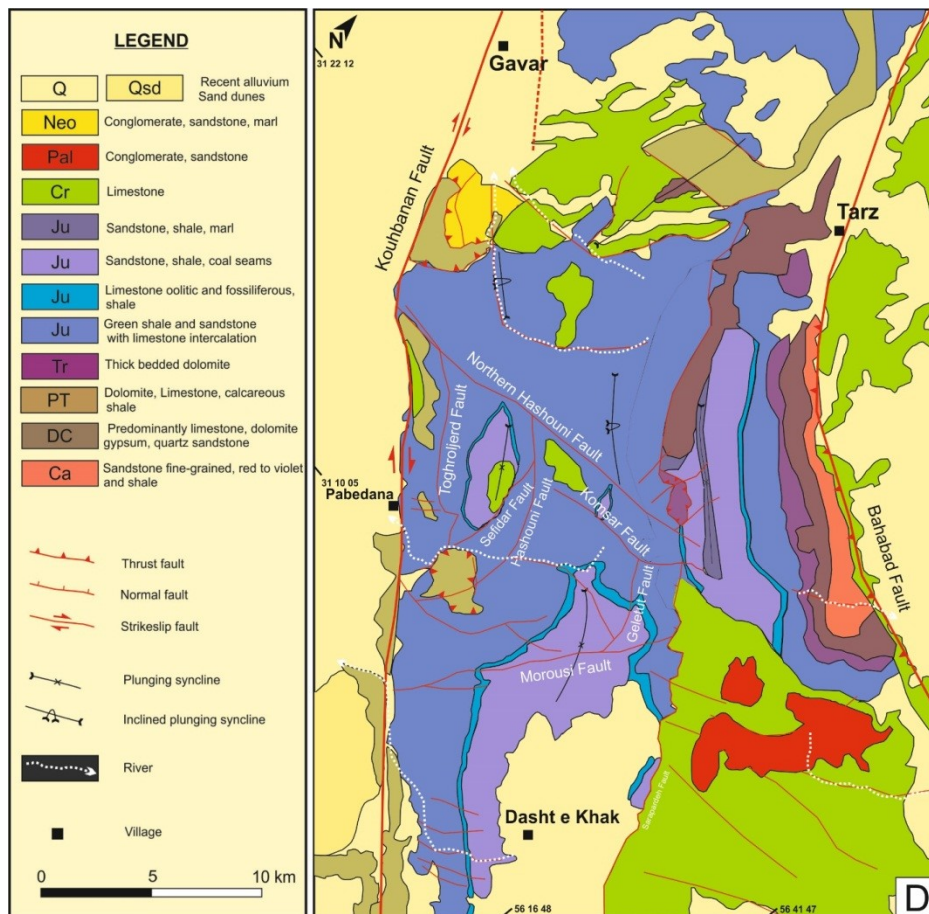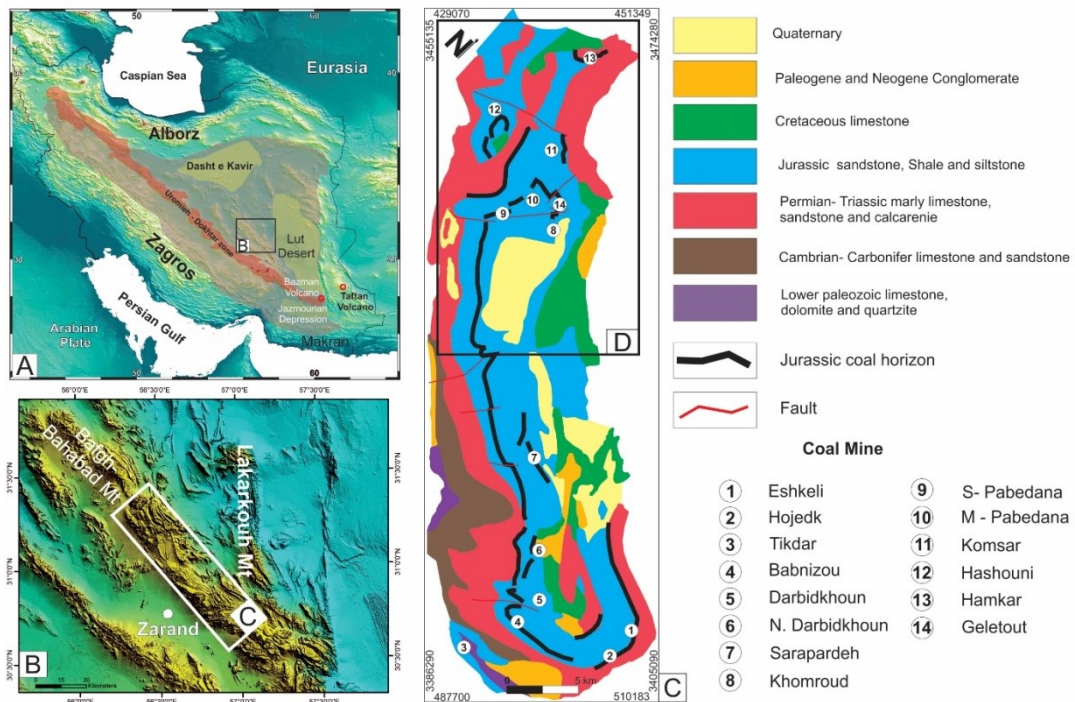
Fig 1. A: Map of the structural- sedimentary classification of Iran. B: The Kerman coal province (KCP) on SRTM map. C: Geological map of KCP. Studied area shown in rectangle (Detailed in D). Modified after Technoexport (1969).

Formation and evalution of Kerman-Behabad coal Synclinorium is related to early kimmerian and laramide to alpine orogenic phase (Technoexport 1969). The mentioned orogenic phases caused folding and numerous faulting in the most sandstone and shale units in the area.

In terms of stratigraphy in the Kerman syncline (Fig 2), Paleozoic sedimentary basin, such as any other place in Iran, are similar to platform shallow deposits. The study of the stratigraphy of this syncline, reveals the Mesozoic sedimentary sequence. This sequence has been started with the marine continental shelf of lower Triassic shale sediments. Middle Triassic carbonates of the Shotori Formation with a significant facies (Dolomite) changed due to the orogenic phase of early Cimmerian become varied to siliciclastic rocks (Sandstone and shale) of the Shemshak group (Technoexport 1969). The Norian-Rhaetian Sea Marine Environment (Nayband Formation), due to the uplifting of the early Cimmerian phase, becomes a non-marine environment of coaly siliciclastic rocks (Abhaaji Formation) on the Jurassic-Triassic border, ammonite compact limestone (Toarcian-Bajocian) represents a development of marine environment, that they have accumulated due to the tensile- compression incident of middle Bajocian. Then, the high thickness of coal siliciclastic rocks of hojedk Formation represents a large sedimentation of the basin and traction in the upper middle Jurassic (Technoexport 1969). Tensile- compression incident of middle cimmerian reaches its peak, in middle Bajocian and as a result, the middle jurassic discontinuity that has been accompanied by lack of precipitation, causes the separation of the Shemshak group from the Bidou Group. Bidou formation was deposited as a result of sedimentation continuing, and following that marls and retrograde marly limestone was appeared in the shallow marine environment and lagoon, the beginning of the block faulting was occurred in the upper Cimmerian and caused the deposition of evaporation and red layers of the Ravar Formation, with the progressing of cretaceous sea, pectin and rudistic limestone of cretaceous in vast areas of the syncline was deposited, and now they have created high altitudes in the syncline (Technoexport 1969).

3. Approach

The northern part of the KCP, as complex area is containing from fracture and faulting due to the operation of various orogenic phases (Fig3). In table 1, the geometric and kinematic characteristics of the main faults of the study area are presented. Strike, length and displacement of faults measure from field observation and by satellite images processing (Fig 4). In our study area, the average number of faults per unit area (km^2) or the surface effect of longitudinal accumulation of faults per unit area (surface faulting intensity) are different. According to the fractures map, almost faults are confined between the two major faults: The Kouhbanan fault in the southwest and Tarz fault in the the northeast.
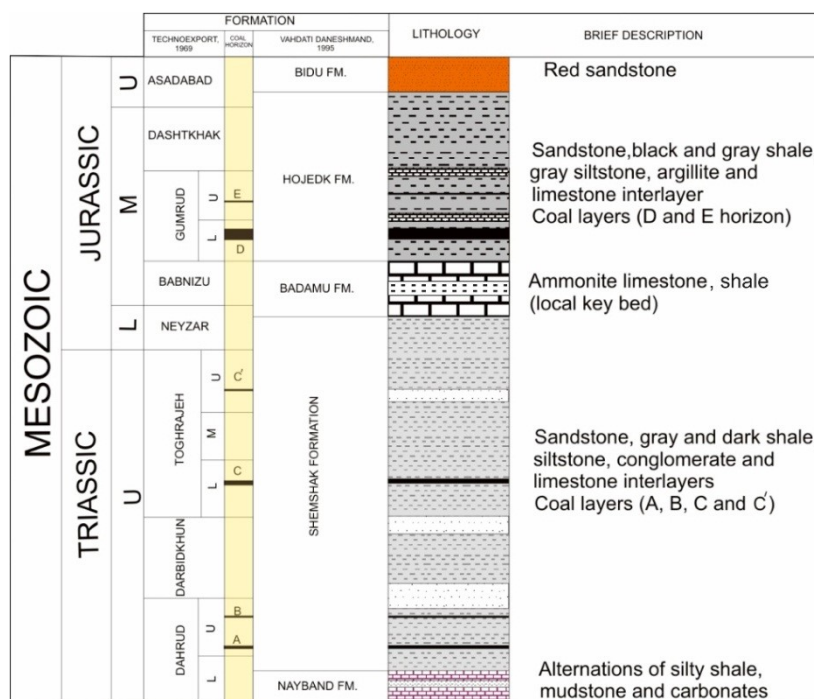

Fig 2. The upper Triassic- Jurassic stratigraphic correlation (Vahdati daneshmand 1995 and Technoexport 1969) and situation of coal seams (Modified after Amiri and Daftarian 2015).

Table 1. Geometric and kinematic characteristics of the main faults in the study area.

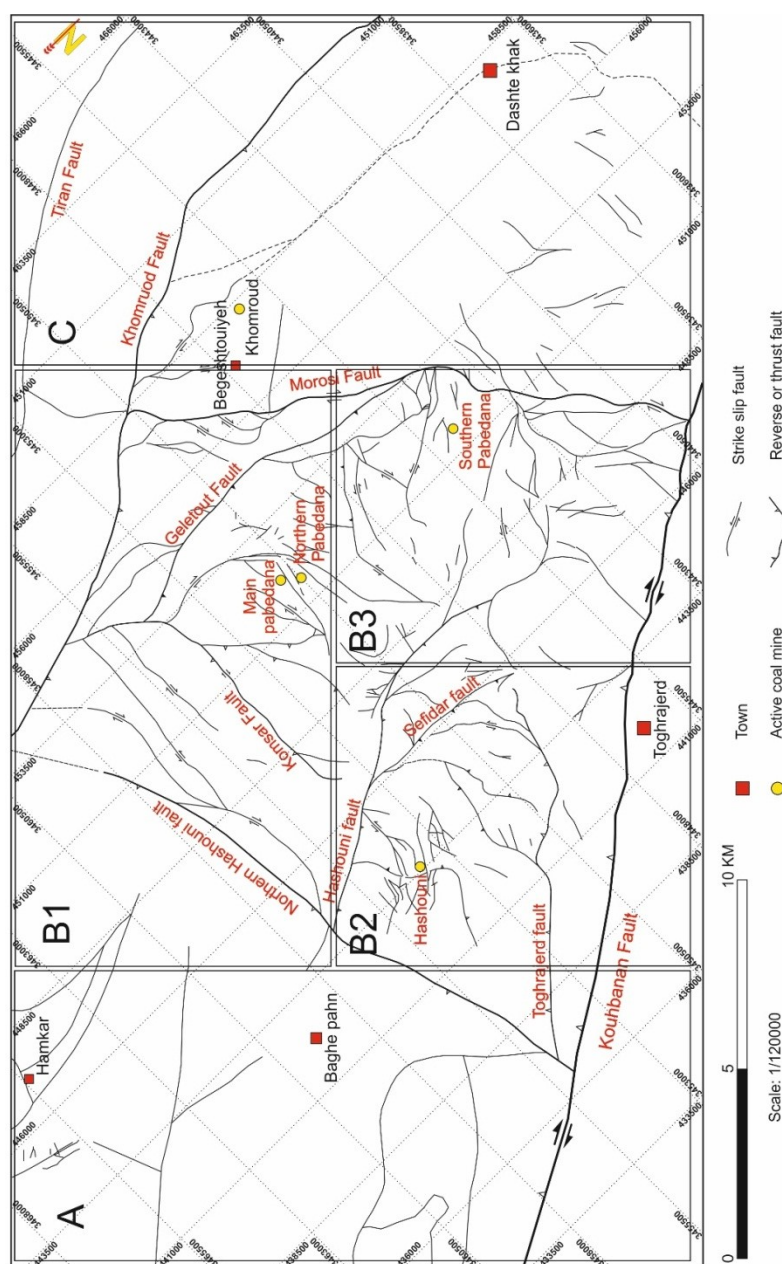| No	Fault name	Length(m)	Azimuth	Displacement(m)	Fault type
1	North Hashouni	16000	80	200	R
2	Toghroljerd	19000	165	1000	R
3	Komsar	10000	85	125	RR
4	Hashouni	11000	156	550	SR
5	Sefidar	5000	5	400	RR
6	Geletout	11000	173	600	RR
7	Morousi	18000	50	200	SR
8	Khomroud	20000	157	400	R
9	Bidengoun	15000	5	200	SR
10	Kouhbanan	40000	142	≤1000	SR
11	Tarz	18000	155	≤1000	SRR

Fig 3. Map of the main faults and fractures in the Northern part of the Kerman Coal province and the classification of the studied area is based on the density of surface fault trace (for further explanation see the text). The main coal mines are marked with yellow circles and residential areas with red quadrants.
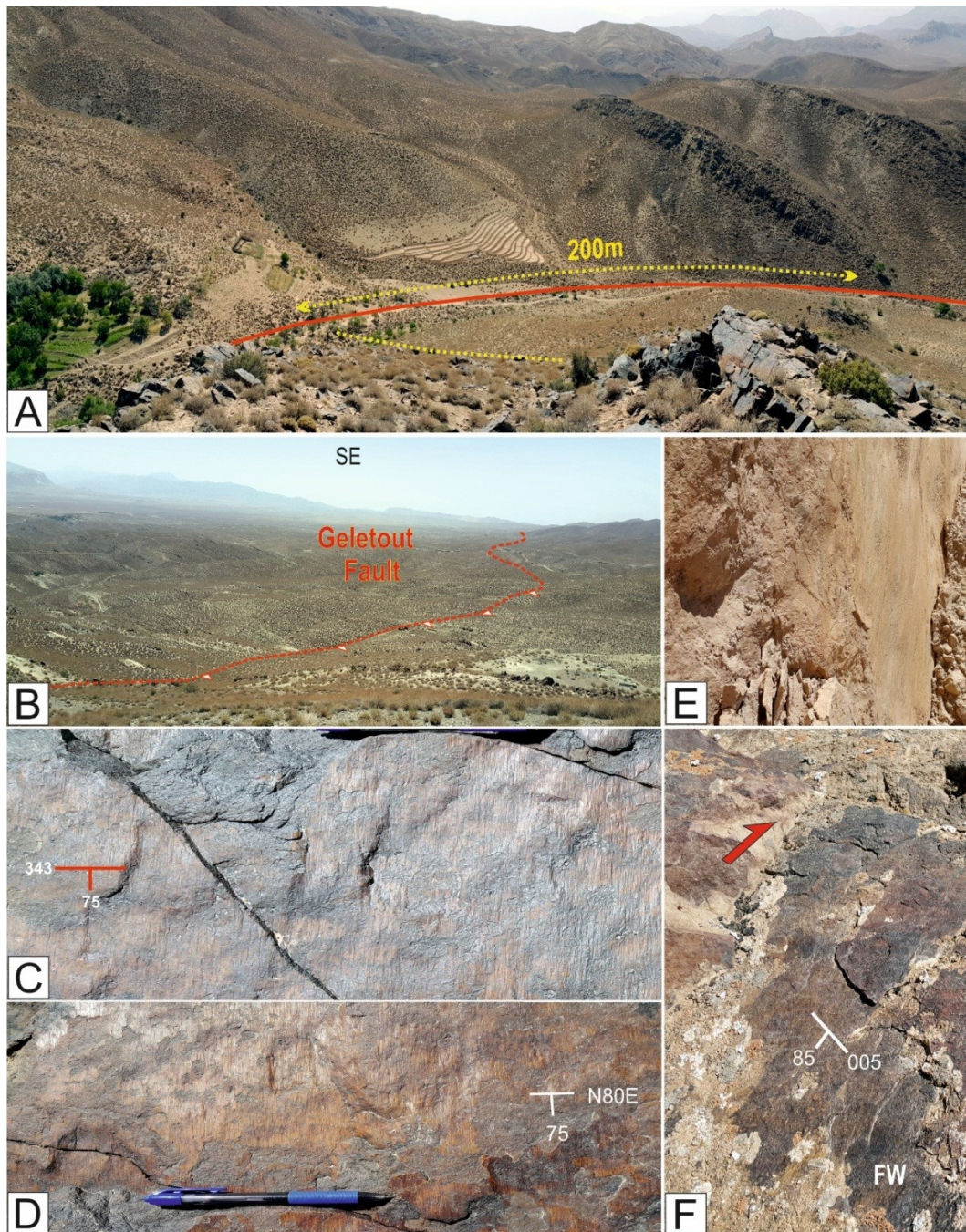
Fig 4. Field photos from faults in the study area. A: displacement in the Morousi fault. B: Scarpment and fault trace of the Geletout fault. C: Hashouni fault D: Fault plane of the Northern Hashouni fault. E: Khomroud fault and F: Close view of the Sefidar fault plane

In study area, density of trace fault (surface density) is high between Northern Hashouni and Morousi faults. Therefore, it can be divided into 3 regions (A, B and C. Fig 3). The B region divided to three Subdomain of B_1, B_2 and B_3 because has a highest fault surface density. The characteristics of the 11 major faults in study area were studied (Table 1). In order to investigate the strike of faults, after plotting the fracture maps and georeferencing, using the Fabric 8 software, a rose diagram of faults strike in each region was prepared (Fig 5). As shown in Fig 5, 27 faults strike shown in zone A, that often have a N-NW trend with a % 30.3 rate of 320 to 340 degrees and a lower percentage (21.2%) in trends of 340 Up to 360°, there are also two other subordinate strikes of 0-10° and 65-75° with similar percentages of 14.8% in this area. 38 faults were identified that often have a strike of northeast-southwest with the highest strike (25.7%) along 70°- 80° strikes in the B_1 zone.

The strike rose diagram of 37 faults were plotted in B₂ zone, and show a highest percentage of strikes (21.8 %) in 320-330 degrees, while the trend of 290-300 ° with the next level with 15.2%, had the most extended strike. In the B₃ zone, strikes of 50 faults were entered into the graph and as shown in the diagram, almost all of the strikes are visible in this subarea. But the highest percentage of strikes is related to trends of 300-310 and 320-330 with value of 14.3% and then to 50°- 60° and 80°- 90° with values of 11.6% and 9.8% respectively. In C zone, the diagram of 19 faults strike was drawn and it was determined that the highest percentage of strikes (31.2%) was related to the trends of 0- 5° and then 25% related to strikes of 333-338°. In this area, EW trends have allocated themselves up to 9% of strikes.

The fracture density in three zones (A, B and C), is determined by the area of the region and length of faults trace in unit area by ArcGIS software and Field works and is presented in Table 2.

3.1. Analysis of the length versus Strike of faults (LvS)

Rose diagrams for faults, that have specified length and relative direct strike, were studied (Fig 6). As can be seen, the equation between length and strike parameters as (y=0.0478x+11.54) that has been calculated to be R = 0.3. There are 2 dominant strike orientation. Domain A with Azimuths at 140°-173° and domain B with Azimuths at 30°-105°.
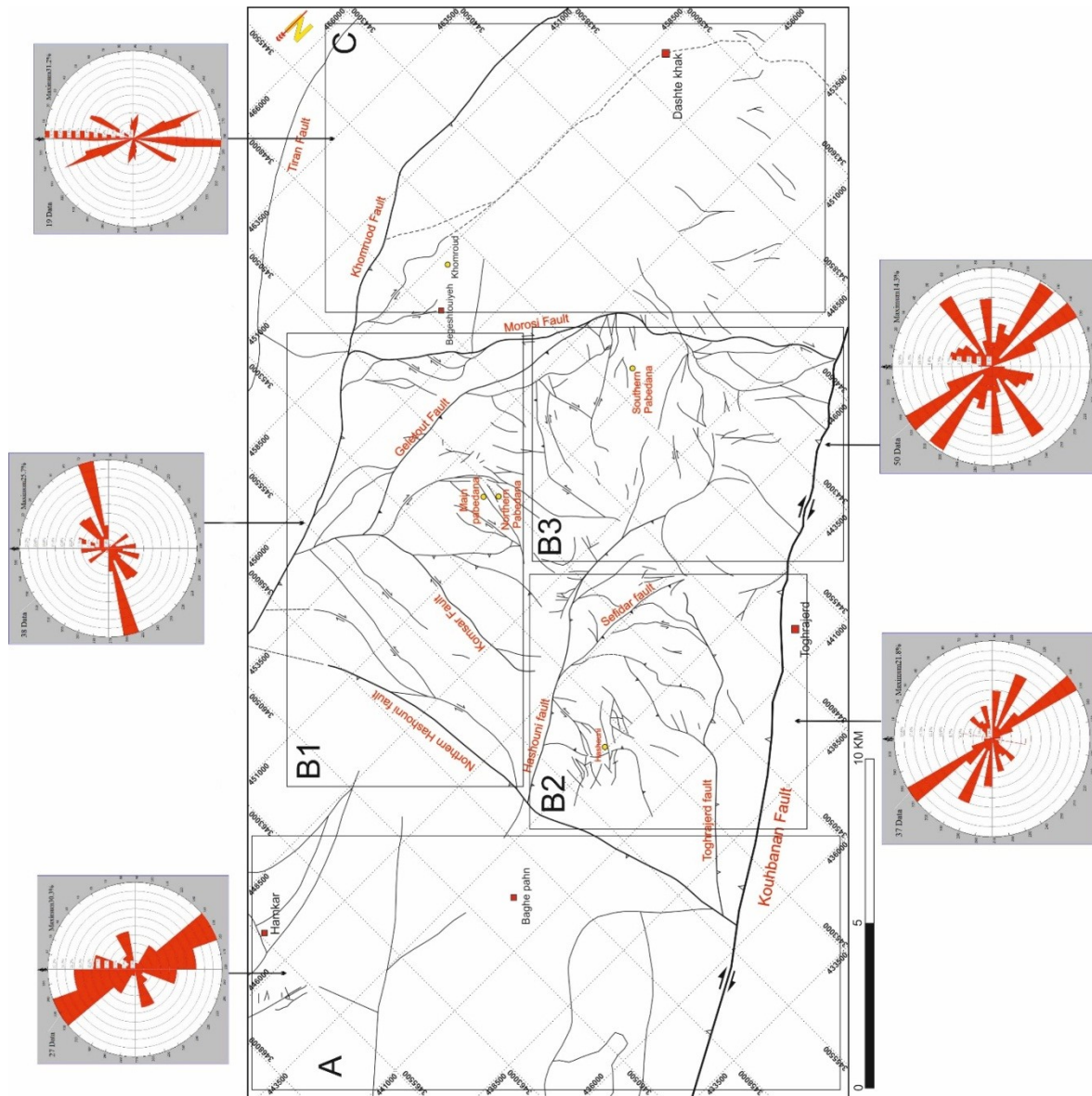

Fig 5. Rose diagrams of faults strikes in the study areas

Table 2. Table of fault surface density and computational parameters.

Zone	Sub Zone	Perimeter (Km)	Area (Km^2)	Accumulation Length (Km)	Surface Density (1/Km^2)		Number of Faults
A	-	55	157	76	0.48		27
B	B$_1$	44	111	108	0.97		38
	B$_2$	34	74	89.5	1.2	1.00	37
	B$_3$	35	76	64	0.84		50
C	-	54	164	43.5	0.26		19

3.2. Analysis of the strike versus displacement of faults (SvD)

In order to the calculation the SvD parameter, the characteristics of 14 faults (including major faults) were used (Fig 7). Measurements of displacement were done by fieldwork as well as observation and processing of satellite images. The equation between the mentioned parameters is calculated as (y=268X+147.4) and the dependence rate is obtained with the value of (R=0.65). We write the power relation between the strike and displacement ($D_{Max} = aoS^{a1}$) according to the general formula ($y = a_0X^{a1}$) the values of a_0 and a_1 are equal to 171.16 and 0.170 respectively, the effective value (deviation) of 2.451 (obtained Fig7). Accordingly, the power relationship between the strike-displacement

parameters can be written as y=171.16X$^{0.170}$ or D=171.16S$^{0.17}$.

3.3. Analysis of the length (L) versus displacement (D) parameter (LvD)

One of the most important fault-related parameters is the LvD, which has been investigated by numerous researchers (for example: Cowie and Scholz 1992; Kim and Sanderson 2005; Schultz et al. 2013). In order to obtain the relationship between the L and D parameters, the characteristics of 20 faults were used, and the statistical diagram is shown in Fig 8. yielded power law relationship between these parameters is (y= 243.58 x$^{0.0336}$). The R value is 0.022, which does not show significant dependence.
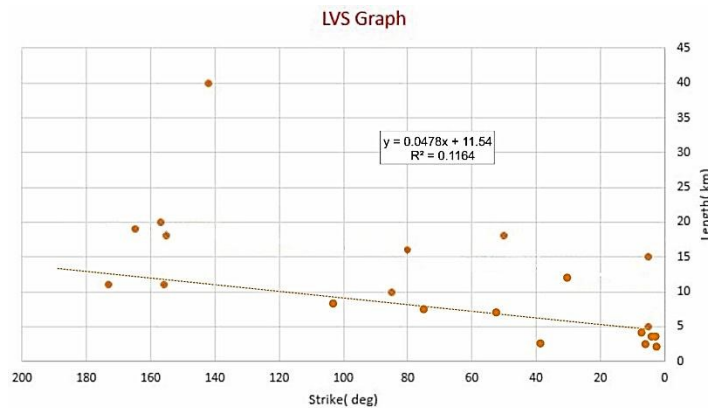

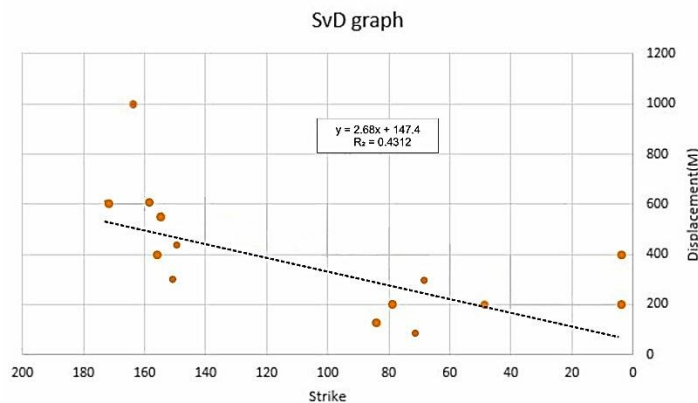Fig 6. Length - strike diagram for major faults in the study area

Fig 7. Displacement - strike diagram for the major faults in the study area
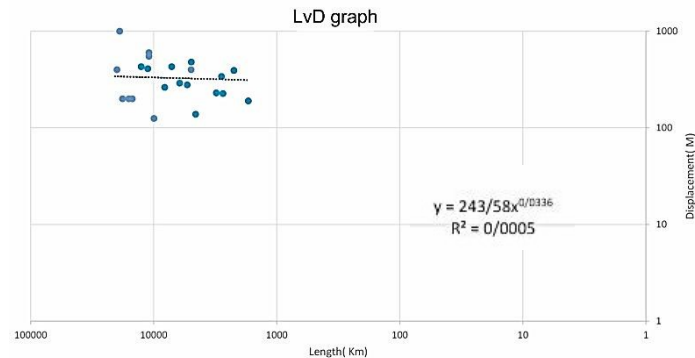
Fig 8. Length-displacement diagram for the major faults in the study area

4. Discussion

The statistical analysis of geometric-kinematic fault properties in the northern part of the Kerman Coal province, includes the points that are discussed below.

The formation of fault systems in different stress condition is due to the variation of their response to stress regimes and their brittleness index (BI) (Nejati and Moosavi 2017). Physical and mechanical characteristic of rocks assemblage (tensile strength, uniaxial compressive strength and elastic modulus...) has a great influence on the formation, development and density of fault in rock assemblages. Among the rocks, sandstone have a faulting ability more than limestone due to higher brittleness index.

Dominant lithology is limestone in northern and southern parts and is sandstone with shale in the middle part of study area (Figs 1d and 2). Accordingly, density of faults in the middle part is higher than the northwest and southeast of the region. It seems, the performance of four major limiting faults (Kouhbanan, Khomroud, Morousi and northern Hashouni faults), caused more fractures in the middle zone, which is well understood by the faults map (Fig 3). The absence of geometric relationship between faults traces (Figs 1 and 3) shows the asynchronous of the formation and their development (Peacock et al. 2017). But the interesting point is that the density of fractures in the B region is equal to unit $(1 = \sum_{n=1}^{125}(L)/A$) and is higher than, A and C parts. Also, according to calculations the density for each of the three sub sites, B_1, B_2 and B_3 is close to 1 (+_ 0.2) (See to Table 2).

Increasing the density of fractures and faulting in this area may be attributed to the complex geological structures, the formation of early faults in this region, and long-term progressive deformation, The density of faults in each sub zone is affected by major faults and in relation to its displacement positioning and geometric relationship (Fig 3). The shear strain focusing in middle of study area and friction slipping with the faulting, may be considered as another effective factor in the high concentration of faults in the middle part. Investigating the length versus strike parameter and the distribution of data shows, faults with different lengths (from 3 to 40 kilometers) at certain angles and at an average angle of 60 degrees has relative to each other (see Fig 6). A series of north-south faults have a lower strike deviation and eastern-western faults have more in strike scattering. Yielded regression, show moderate dependence between the length and the strike. This may be occur due to the synchronous study of strike slip faults (Such as: Morousi and Komsar faults) and reverse faults (Such as: Hashouni and Komsar faults) and if they are studied separately, more precise results can be obtained. Another point is that the relationship between the above parameters for large faults has a higher accuracy, especially for faults longer than ten kilometers (For example: Khomroud and Morousi faults. See figs 1D and 3). It should be noted that in some cases, using of back bearing increases the accuracy of the obtained response. The relationship between the strike and displacement along the fault with the regression of (0.6), represents the medium dependency between two parameters. However, the displacement rate varies for two series of faults (NW and NE Strikes), so that in NW faults strike, more movement and cumulative displacement were measured. Also, the range of movement in the first series (NW) is much higher than the second (NE), without considering the main faults of Kouhbanan and Tarz, because they are very old and have a large range of displacement (Walker and Allen 2012) and caused the KCP Triassic-Jurassic sedimentary basin (Technoexport 1969)

Length-displacement relationships can be used to a series fault, for available structures in different rocks, depths, and different locations. These conditions are also occurred due to modulus, ultimate strength and stress intensity change and various host rocks. In other hand, the scaling relationships of faults may be influenced by previous structures. Different mechanisms of deformation that cause heterogeneity and anisotropy of the deformed province for stress performance are also influential in these relationships. Regarding the results in the local scale, the length and displacement of faults with a length of less than 1 km, were not possible to measure because existence of sedimentary cover and the absence of obvious physiographic evidence.

5. Conclusion

Due to the inherent complexity of the faults, there is no consensus on the faults scaling relationships. In the northern part of Kerman coal province which is resulted from the lithological diversity, type of faulting, reversal of tectonic and operating orogenic phases. Analysis of the length-strike and strike-displacement parameters, show a clustering in depicted data which have many similarities to each other. The North-South faults have tighter clustering; this is occurred due to an increase in exponential parameter as the result of the spacing between the measured faults. The density of faults is related to type of rock assemblages and is higher in sandstones, especially in the middle part of study area. The length-displacement relationships of faults for this part of the Kerman Coal province have not shown a dependable dependence, and this may indicate asynchronous of the formation and their development.

References

Amiri A, Daftarian, M (2015) Preliminary Hydrocarbon Potential Evaluation of Hojedk Formation in Kerman Coaly Syncline (KCS), Iran: Geochemical Approach, *Journal of Gas Technology* 1: 28-48

Aydin A, Nur A (1982) Evolution of pull-apart basins and their scale independence, *Tectonics* 1: 11-21.

Aydin A, Berryman JG (2010) Analysis of the growth of strike-slip faults using effective medium theory, *Journal of Structural Geology* 32: 1629-1642.

Childs C, Manzocchi T, Walsh JJ, Bonson CG, Nicol A, Schöpfer MPJ (2009) A geometric model of fault zone and fault rock thickness variations, *Journal of Structural Geology* 31: 117-127.

Cowie PA, Scholz CH (1992b) Displacement-length scaling relationships for faults: data synthesis and

discussion, *Journal of Structural Geology* 14: 1149-1156.

De Joussineau G, Aydin A (2009) Segmentation along strike-slip faults revisited, *Pure and Applied Geophysics* 166: 1575-1594.

Kim YS, Sanderson DJ (2005) The relationship between displacement and length of faults: a review, *Earth-Science Reviews* 68: 317-334.

Kim YS, Peacock DCP, Sanderson DJ (2004) Fault damage zones, *Journal of Structural Geology* 26: 503-517.

Long JJ, Imber J (2011) Geological controls on fault relay zone scaling, *Journal of Structural Geology* 33: 1790-1800.

Nejati H R, Moosavi S A (2017) A new brittleness index for estimation of rock fracture toughness, Journal of Mining & Environment 8: 83-91

Peacock D C P, Nixon C W, Rotevatn A, Sanderson D J, Zuluaga L F (2017) Interacting faults, Journal of Structural Geology 97: 1-22.

Soliva R, Benedicto A (2004) A linkage criterion for segmented normal faults, *Journal of Structural Geology* 26: 2251-2267.

Schultz RA, Klimczak Ch, Fossen H, Olson J, Exner U, Reeves D, Soliva R (2013) Statistical tests of scaling relationships for geologic structures, *Journal of Structural Geology* 48: 85-94.

Technoexport "Soviet Union" (1969) Geological map of the Kerman coal deposits, *National Iranian Steel Company report*, No 1466.

Walker F, Allen M. (2012) Offset rivers, drainage spacing and the record of strike-slip faulting: The KuhBanan Fault, Iran, *Tectonophysics* 530-531: 251-263.

Wesnousky SG (1988) Seismological and structural evolution of strike-slip faults, *Nature* 335: 340-343.